02;13

Sputtering thresholds during ion bombarding of different targets

© P.Yu. Babenko, V.S. Mikhailov, A.N. Zinoviev

Ioffe Institute, St. Petersburg, Russia
E-mail: babenko@npd.ioffe.ru

Received December 22, 2023
Revised February 20, 2024
Accepted March 9, 2024

Collision models leading to an explanation of the position of energy thresholds during sputtering of various materials are analyzed. The totality of available experimental and computational data can be described within the framework of a model that takes into account multiple collisions. An empirical curve is proposed to describe the position of the thresholds over the entire possible range of mass ratios of colliding particles. The strong influence of the shape of the surface potential barrier on the position of the sputtering energy threshold is shown.

Keywords: atomic collisions, sputtering, sputtering energy threshold, surface potential barrier.

DOI: 10.61011/TPL.2024.06.58478.19851

The process of sputtering of materials under ion bombardment is used to clean and etch surfaces, fabricate thin films, and perform surface analysis. Sputtering is the governing factor in destruction of electrodes in electrical equipment and structural materials in plasma facilities. Sputtering processes are being studied extensively [1–7]. Our studies [8–10] were focused on sputtering of Be and W (materials considered to be promising for the construction of the first wall and the divertor of the ITER tokamak) by hydrogen isotopes.

The dependence of sputtering yield Y on energy E_0 of a bombarding particle is threshold in nature (Fig. 1). The curve in Fig. 1 represents the results of our calculation for a planar barrier, while dots correspond to the experimental data from [11]. It should be noted that near-threshold experimental data are extremely scarce [5,12–15]. An exact knowledge of sputtering thresholds is of prime importance for fusion research. With the temperature of ions in near-surface plasma being below the sputtering threshold, a small change in the threshold leads to a dramatic increase in the number of plasma particles involved in sputtering, which may lead to catastrophic failure of the first wall of a tokamak reactor.

To be sputtered, a particle needs to overcome sublimation energy U_s [16] (surface binding energy). It can be seen from Fig. 2 that sublimation energies vary rather widely. They exert a significant influence on the process of sputtering. The case of normal incidence of a beam onto a target is examined in the present study.

Two distinct cases need to be considered for a surface potential barrier preventing the escape of a particle from a target: if this barrier is spherical, the escape condition is written as $E_2 > U_s$ [17], while the condition for a planar potential barrier (smooth surface) changes to $E_2 \cos^2\theta > U_s$ [17], where E_2 is the energy of a sputtered particle and θ is the angle of particle escape relative to the normal to the surface. Figure 3, *a* presents the experimental results from [12,14,15], the data from [11] obtained via computer modeling for a planar potential barrier, and the results of our calculation for two types of a surface potential barrier.

Energy E_2 transferred in collision by a scattered particle to a target atom is

$$E_2 = E_0\gamma\cos^2\theta_1, \quad \gamma = \frac{4M_1M_2}{(M_1+M_2)^2}, \qquad (1)$$

where θ_1 is the scattering angle of the recoil particle. The dependence of parameter $P = \gamma E_{th}/U_s$ (E_{th} is the threshold energy) on ratio M_2/M_1 is shown in Fig. 3, *a*.

It can be seen from Fig. 3, *a* that the experimental data are scattered widely between the results of our calculations for two limit cases of a surface potential barrier. The data of our calculation for Be and W targets agree closely. In region $M_2/M_1 < 1$, the calculated data of Behrisch [11] for a planar potential barrier lie 16% higher than the results of our

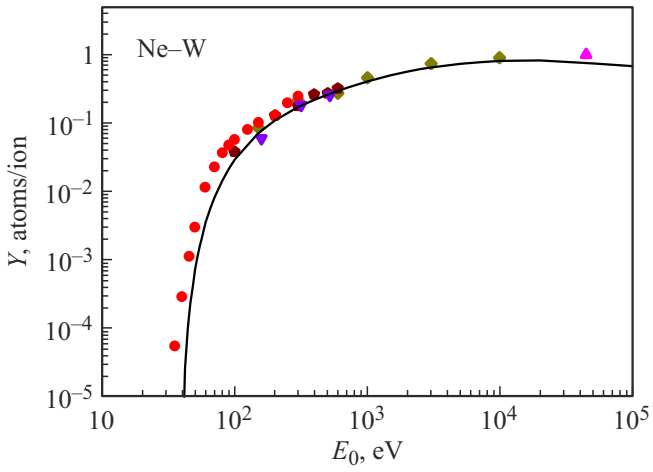

Figure 1. Sputtering yield Y for a tungsten target and bombarding Ne atoms as a function of their energy E_0. The curve is the result of our calculation for a planar barrier. Dots represent the experimental data taken from [11].

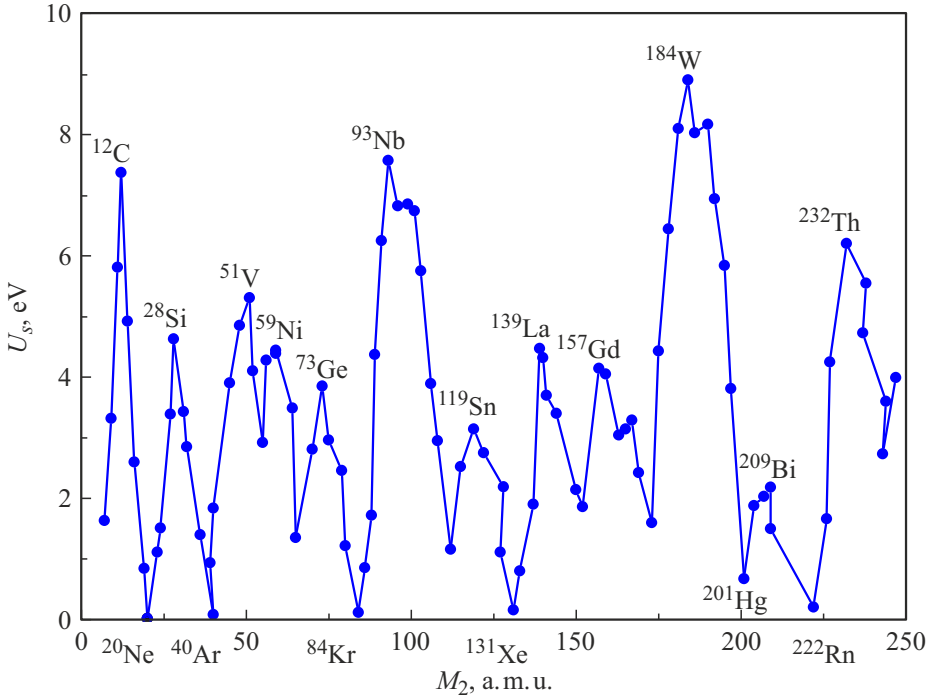

Figure 2. Sublimation energies for different materials [16].

calculation. At $M_1 > M_2$, a bombarding particle transfers its energy to numerous recoil particles. In a subsequent cascade of collisions, a particle with its energy exceeding the surface binding energy escapes from the surface and is regarded as a sputtered one. The process of sputtering is characterized in this case by the cascade Sigmund theory [17]. In the $M_1 < M_2$ case, the sputtering mechanism changes, and the contribution of sputtering of surface layers by a flux of backscattered particles becomes significant. A theoretical description of this case was presented in [18]. Condition $E_{th} = U_s/[\gamma(1-\gamma)]$ (i.e., $P = 1/(1-\gamma)$) was proposed for the threshold energy in [19]. It follows from Fig. 3, *a* that this formula remains adequate at $M_2/M_1 > 5$.

Let us examine the case of a spherical potential barrier and $E_2 > U_s$. In scattering by angle β, energy E_1 of a bombarding particle is written as

$$\frac{E_1}{E_0} = \left[\frac{M_1}{M_1+M_2}\right]^2 \times \left(\cos\beta \pm \left\{\left(\frac{M_2}{M_1}\right)^2 - \sin^2\beta\right\}^{1/2}\right)^2 = K_1(\beta), \qquad (2)$$

where E_0 is the energy of a bombarding ion; M_1 and M_2 are the masses of a bombarding ion and a surface atom, respectively; and β is the scattering angle. If a bombarding particle gets scattered off a surface layer, a recoil particle propagates into the bulk of a target and may contribute to sputtering only via a cascade of collisions with other target atoms. Let us consider a bombarding particle that propagates over distance d within the target and gets scattered by angle β; in doing so, it should turn by angle greater than 90° and knock out a surface atom. In this case, $E_1/E_0 \leqslant (M_2-M_1)/(M_2+M_1) = (1-\gamma)^{0.5}$ and sputtered particle energy $E_2 = \gamma E_1 = \gamma(1-\gamma)^{0.5}$. Let us introduce a correction for the energy loss related to electronic stopping of a bombarding particle in back-and-forth propagation over interparticle distance d within the target. In this case, $E_1 = (1-\gamma)^{0.5}E_0 - dE/dx \cdot 2d$ and $E_2 = \gamma E_1 > U_s$. Here, dE/dx are the electronic stopping powers for threshold energy E_{th}. The expression for parameter P is

$$P = \frac{\gamma E_{th}}{U_s} = (1-\gamma)^{-0.5}\left(1 + \frac{\gamma}{U_s}\frac{dE}{dx}2d\right). \qquad (3)$$

It can be seen from Fig. 3, *b* that the model of a single collision provides an adequate fit to the data for a spherical barrier only at $M_2/M_1 > 10$. As is known, the energy lost by a particle in the case of a double collision and scattering by angle $\beta/2$ is lower than the energy lost in single scattering by angle β. If the overall turn angle of a fast particle is fixed, the energy loss is minimized when scattering angles are equal and both scattering events proceed in the same plane. Formula (3) takes the following form for double scattering in this case:

$$P = \gamma\frac{E_{th}}{U_s} = \frac{1}{K_1^2(\beta)} \times \left(1 + \frac{\gamma}{U_s}\frac{d}{\sin\beta}\left(\frac{dE}{dx}(E_1) + K_1(\beta)\frac{dE}{dx}(E_0)\right)\right). \qquad (4)$$

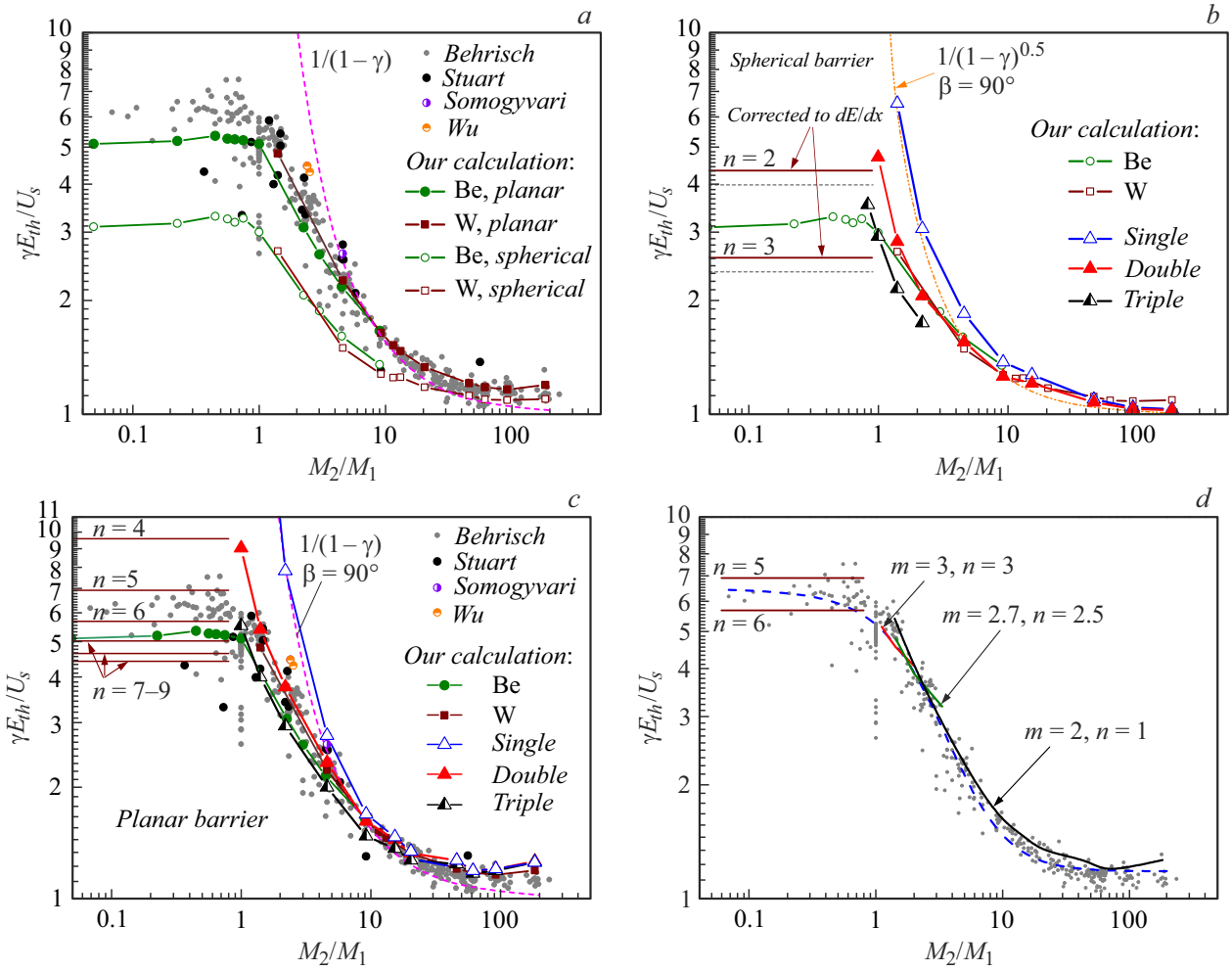

Figure 3. Dependence of parameter $P = \gamma E_{th}/U_s$ on mass ratio M_2/M_1. *a* — Results of computer modeling for a planar potential barrier from [11], results of modeling with our program for planar and spherical barriers, and experimental data from [12,14,15]. *b* — Spherical potential barrier: data obtained in computer modeling with our program and estimates provided by formulae (3) and (4). *b* — Planar potential barrier: results of computer modeling from [11], results of modeling with our program, estimates obtained using formula (5), and experimental data from [12,14,15]. *d* — Empirical curve characterizing the entire set of processed data (6). Segments of curves corresponding to different values of collision multiplicity m of a bombarding particle and collision number n of target atoms are shown.

Here, $dE/dx(E_1)$ and $dE/dx(E_0)$ are the electronic losses for bombarding particle energies E_1 and E_0, respectively, and $K_1(\beta)$ was described above (see (2)). Analyzing the variation of kinetic energy and deceleration by target electrons within different segments of the trajectory, one may obtain an expression for arbitrary collision multiplicities m and n of bombarding and target particles, respectively.

It can be seen from Fig. 3, *b* that the model of double scattering ($m = 2$) provides a close fit to the data for a spherical barrier at $M_2/M_1 > 1.5$. At $M_2 \approx M_1$, a contribution from triple collision ($m = 3$) is possible.

The cascade mechanism is dominant at $M_2/M_1 < 1$. A bombarding particle transfers energy $\gamma E_0 \cos^2\theta_1$ to a recoil atom, where θ_1 is the recoil atom scattering angle. In a subsequent cascade, colliding particles have equal masses. After the first collision of this kind, the energy of the second particle is $E_2 = \gamma E_0 \cos^2\theta_1 \cos^2\theta_2$. The product of cosines reaches its maximum value at $\theta_1 = \theta_2 = \theta$ if sum $\theta_1 + \theta_2$ is fixed. We assume that $\theta_1 + \theta_2 \geqslant 90°$. Thus, $E_2 = 0.25\gamma E_0 = U_s$ and $P = \gamma E_{th}/U_s = 4$. In a triple collision, $\theta = 30°$ and $P = 1/\cos^6\theta = 2.37$. The value of P increases if the correction for particle electronic stopping is introduced. At $n = 2$, $P = 4.36$; at $n = 3 - P = 2.58$.

In the case of a planar barrier, the escape condition for a sputtered particle changes to $E_2 \cos^2\theta \geqslant U_s$. In single scattering, $E_2 = \gamma E_0 K_1(\beta)$; i.e., $\gamma E_0 K_1(\beta)\cos^2\theta \geqslant U_s$. The maximum value of energy E_2 corresponds to a head-on collision. Therefore, $\theta = \pi - \beta$. We seek the maximum value of parameter $K_1(\beta)\cos^4\beta$ at $\beta > \pi/2$. It is attained at $\beta = \pi$. Next, we introduce the correction for electronic stopping of a bombarding particle in the target. It can be seen from Fig. 3, *c* that single scattering does not provide an adequate fit to the data at $M_2/M_1 < 10$. The introduction of double and triple scattering yields P values that lie close

Dependence of parameter $P = \gamma E_{th}/U_s$ on the number of collisions without and with account for the correction for deceleration by target electrons

n	P	θ, °	P_{cor} (Be)			P_{cor} (W)		
			$\alpha = 1.5$	$\alpha = 1$	$\alpha = 0.5$	$\alpha = 1$	$\alpha = 0.7$	$\alpha = 0.5$
2	64	60	66.2	65.5	64.7	66.9	66.1	65.5
3	16	45	17.9	17.3	16.6	18.6	17.8	17.3
4	8.33	36	10.2	9.58	8.94	10.9	10.1	9.59
5	5.62	30	7.63	6.93	6.26	8.40	7.50	6.94
6	4.31	25.7	6.46	5.70	4.98	7.31	6.32	5.71
7	3.55	22.5	5.87	5.03	4.26	6.81	5.72	5.05
8	3.06	20	5.57	4.65	3.82	6.62	5.41	4.67
9	2.73	18	5.44	4.43	3.53	6.60	5.26	4.45
10	2.48	16.4	5.41	4.31	3.34	6.69	5.21	4.33
11	2.30	15	5.46	4.26	3.20	6.87	5.24	4.28

to the discussed data at $M_2/M_1 > 1.4$. In the vicinity of $M_2 \approx M_1$, triple scattering provides a better description of the analyzed data. The introduction of the correction for electronic stopping leads to an increase in P and allows one to obtain a closer fit to the analyzed data at $M_2/M_1 < 10$. Note that the $P = 1/(1-\gamma)$ curve proposed earlier goes 20% lower at $M_2/M_1 > 50$.

Let us examine the curve behavior in the region of operation of the cascade mechanism with a planar potential barrier. Energy ratio E_1/E_0 in a single elastic collision of a fast particle is characterized by quantity $K_1(\beta)$. Since target particles have equal masses, the energy ratio in a single collision of two target particles is characterized by quantity $\cos^2\beta$, where β is the trajectory turn angle. At $M_2/M_1 < 1$, $\cos^2\beta > K_1(\beta)$; therefore, the minimum energy loss in the examined case is achieved in cascades involving target particles, and the energy loss in the contrary case (at $M_2/M_1 > 1$) is lower in cascades involving fast particles.

In the first collision, a fast particle transfers energy to a target particle: $E_1 = E_0\gamma\cos^2\beta$. Since angle β is always smaller than 90°, another collision (or several collisions) of target particles is needed for a particle to escape from the target. Analyzing a collision cascade and taking the particle escape condition for a planar barrier into account, we find $E_2\cos^2\theta = \gamma E_0\cos^4\beta\cos^2\theta \geqslant U_s$. Escape angle θ of a sputtered particle is measured from the normal to the surface, and $\theta = \pi - 2\beta$. The threshold energy is maximized at $\beta = \theta = 60°$. In double scattering, $P = \gamma E_{th}/U_s \geqslant 64$. In triple scattering, $\gamma E_0\cos^8\theta \geqslant U_s$, $\theta \geqslant 45°$, and $\gamma E_{th}/U_s \geqslant 16$. The formula for n-fold scattering is

$$P = \gamma\frac{E_{th}}{U_s} > \frac{1}{\cos^{2(n+1)}\theta}. \qquad (5)$$

The values of P are listed in the table. In a model with elastic collisions only, P continues to decrease with an increase in scattering multiplicity. The quantity corrected for particle energy loss due to electronic stopping is designated as P_{cor}. The values of specific electronic energy loss dE/dx were taken from SRIM tables [20]. These dE/dx value were multiplied by correction factor α. It can be seen from the table that the introduction of inelastic losses slows down the reduction of P_{cor} at higher n and leads to saturation of this dependence on the number of collisions at large n and arbitrary values of α. A close fit to the analyzed data is achieved at $n \approx 5-7$.

Figure 3, *d* presents the empirical curve that was obtained by parameter fitting with the aim of obtaining the closest agreement with processed data. The formula for this curve is

$$\gamma\frac{E_{th}}{U_s} = \frac{5.56}{1 + 0.164\left(\frac{M_2}{M_1} + 0.509\right)^2} + 1.177. \qquad (6)$$

The entire set of data is characterized well with curve segments corresponding to varying collision multiplicities m of a bombarding particle and collision numbers n of target atoms (Fig. 3, *d*).

Thus, the dependence of the threshold position on the mass ratio of colliding particles is attributable to differences in the mechanism of sputtering at $M_2/M_1 < 1$ and $M_2/M_1 > 1$. At $M_2/M_1 < 1$, the role of a bombarding particle is reduced to transferring energy to target particles. The positions of thresholds are specified by a cascade of $n \approx 5-7$ collisions of target particles. At $M_2/M_1 > 1$, collisions of a bombarding particle with target atoms produce a flux of backscattered atoms, which collide with atoms in the surface layer to induce sputtering. Triple and double scattering of a bombarding particle produces a significant contribution at $1 < M_2/M_1 < 2$. The model of single scattering provides a fine description of the analyzed data at $M_2/M_1 > 10$ if the energy loss related to particle deceleration by target electrons is taken into account.

Conflict of interest

The authors declare that they have no conflict of interest.

References

[1] A.P. Mika, P. Rousseau, A. Domaracka, B.A. Huber, Phys. Rev. B, **100** (7), 075439 (2019). DOI: 10.1103/PhysRevB.100.075439

[2] A. Tolstogouzov, P. Mazarov, A.E. Ieshkin, S.F. Belykh, N.G. Korobeishchikov, V.O. Pelenovich, D.J. Fu, Vacuum, **188**, 110188 (2021). DOI: 10.1016/j.vacuum.2021.110188

[3] F. Duensing, F. Hechenberger, L. Ballauf, A.M. Reider, A. Menzel, F. Zappa, T. Dittmar, D.K. Bohme, P. Scheier, Nucl. Mater. Energy, **30**, 101110 (2022). DOI: 10.1016/j.nme.2021.101110

[4] A. Lopez-Cazalilla, F. Granberg, K. Nordlund, C. Cupak, M. Fellinger, F. Aumayr, W. Hauptstra, P.S. Szabo, A. Mutzke, R. Gonzalez-Arrabal, Phys. Rev. Mater., **6** (7), 075402 (2022). DOI: 10.1103/PhysRevMaterials.6.075402

[5] P. Phadke, A.A. Zameshin, J.M. Sturm, R. van de Kruijs, F. Bijkerk, Nucl. Instrum. Meth. Phys. Res. B, **520**, 29 (2022). DOI: 10.1016/j.nimb.2022.03.016

[6] N.N. Andrianova, A.M. Borisov, E.S. Mashkova, V.I. Shulga, J. Surf. Investig., **10** (2), 412 (2016). DOI: 10.1134/S1027451016020233.

[7] V.I. Shulga, J. Surf. Investig., **14** (6), 1346 (2020). DOI: 10.1134/S1027451020060440.

[8] P.Yu. Babenko, V.S. Mikhailov, A.N. Zinoviev, Tech. Phys. Lett., **49** (4), 80 (2023). DOI: 10.21883/TPL.2023.04.55887.19432.

[9] P.Yu. Babenko, V.S. Mikhailov, A.P. Shergin, A.N. Zinoviev, Tech. Phys., **68** (5), 662 (2023). DOI: 10.21883/TP.2023.05.56074.12-23.

[10] V.S. Mikhailov, P.Yu. Babenko, A.P. Shergin, A.N. Zinov'ev, JETP, **137** (3), 413 (2023). DOI: 10.1134/S106377612309011X.

[11] R. Behrisch, W. Eckstein, *Sputtering by particle bombardment* (Springer, Berlin, 2007). DOI: 10.1007/978-3-540-44502-9

[12] R.V. Stuart, G.K. Wehner, J. Appl. Phys., **33** (7), 2345 (1962). DOI: 10.1063/1.1728959

[13] R.P. Doerner, D.G. Whyte, D.M. Goebel, J. Appl. Phys., **93** (9), 5816 (2003). DOI: 10.1063/1.1566474

[14] Sh.-M. Wu, R. van de Kruijs, E. Zoethout, F. Bijkerk, J. Appl. Phys., **106** (5), 054902 (2009). DOI: 10.1063/1.3149777

[15] Z. Somogyvari, G.A. Langer, G. Erdelyi, L. Balazs, Vacuum, **86** (12), 1979 (2012). DOI: 10.1016/j.vacuum.2012.03.055

[16] C. Kittel, *Introduction to solid state physics*, 8th ed. (Wiley, N.Y., 2005).

[17] P. Sigmund, Phys. Rev., **184** (2), 383 (1969). DOI: 10.1103/PhysRev.184.383

[18] G. Falcone, Riv. Nuovo Cim., **13** (1), 1 (1990). DOI: 10.1007/BF02742981.

[19] R. Behrisch, G. Maderlechner, B.M.U. Scherzer, M.T. Robinson, Appl. Phys., **18** (4), 391 (1979). DOI: 10.1007/BF00899693

[20] *SRIM — The stopping and range of ions in matter*. http://srim.org

Translated by D.Safin